Journal of Pharmaceutical Investigation (2023) 53:417–426
https://doi.org/10.1007/s40005-023-00613-2

ORIGINAL ARTICLE

# Orodispersible film incorporating nanoparticulate loratadine for an enhanced oral bioavailability

Khanh Van Nguyen[1] · Thu Kim Dang[1] · Linh Thi Dieu Vu[1] · Nhan Thi Ha[2] · Hieu Duy Truong[3] · Tuan Hiep Tran[2]

Received: 18 November 2022 / Accepted: 28 January 2023 / Published online: 21 February 2023


## Abstract

**Purpose** Loratadine (LOR), a commonly prescribed antihistamine, has low water solubility but high permeability. In this study, an orodispersible film incorporating the nanoparticulate loratadine was prepared to enhance the oral bioavailability of a poorly water-soluble drug.

**Methods** Nanoparticulate loratadine was formulated using the antisolvent precipitation method and optimized by a single-factor design based on the particle size and polydispersity index. The optimal formulation was spray-dried and characterized by powder X-ray diffraction and differential scanning calorimetry. Nanoparticulate loratadine was loaded into an orodispersible film using a solvent casting method.

**Results** In the dissolution tests, the nanoparticulate loratadine-loaded orodispersible film exhibited a 6.5-fold higher dissolution rate than the pure loratadine-loaded film and a similar dissolution rate compared to the commercialized orodispersible tablet, Loratadine SPM. In pharmacokinetic studies conducted on rats, the maximum concentration ($C_{max}$) and area under the curve of the plasma concentration–time profile from 0 to 24 h ($AUC_{0\text{-}24\,h}$) of the nanoparticulate loratadine-loaded orodispersible film significantly increased 1.8-fold and 5.8-fold, respectively. The elimination half-life ($t_{1//2}$) increased 5.1-fold compared to the loratadine-loaded counterpart.

**Conclusion** These results suggest the potential of orodispersible films to improve the oral bioavailability of poorly water-soluble drugs and promote compliance in pediatric and geriatric patients.

**Keywords** Loratadine · Orodispersible film · Nanoparticles · Enhancement of bioavailability · Pharmacokinetics

## Introduction

Loratadine (LOR) is one of the most commonly prescribed antihistamine medicines used to treat symptoms of allergies, such as rhinitis, conjunctivitis, and urticaria (Roman and Danzig 1993). This compound is categorized as class II according to the Biopharmaceutical Classification System (BCS) owing to its low water solubility and high permeability (Khan et al. 2004). LOR is a weakly basic compound with a $pK_a$ of 5.2, resulting in pH-dependent solubility and a highly variable pharmacokinetic profile (Khan et al. 2004; Sora et al. 2007). Therefore, several studies have been performed to prepare nanoparticles to improve the dissolution rate and/or bioavailability of LOR, such as solid dispersions (Frizon et al. 2013; Kapote and Wagner 2021), self-microemulsifying drug delivery systems (Frizon et al. 2013; Madhav and Kishan 2018; Desai et al. 2020), co-amorphous systems (Wang et al. 2017), and solid lipid nanoparticles (Üner et al. 2014; Sarheed et al. 2020).

Despite their advantages, nanosizing technologies increase the particle surface area, which leads to poor long-term stability due to agglomeration, crystal growth, changes in the crystalline state, and chemical degradation (Wu et al. 2011). Moreover, these nanoparticulate formulations are primarily liquid, making their shipping difficult. These challenges necessitate further processing of nanoparticles into solid dosage form designs to enhance stability and/or patient convenience (Van Eerdenbrugh et al. 2008).

✉ Tuan Hiep Tran
hiep.trantuan@phenikaa-uni.edu.vn

[1] University of Medicine and Pharmacy, Vietnam National University, Hanoi, Y1 Building, 144 Xuan Thuy, Cau Giay, Hanoi, Vietnam

[2] Faculty of Pharmacy, PHENIKAA University, Yen Nghia, Ha Dong, Hanoi 12116, Vietnam

[3] Quang Binh Pharmaceutical Joint-Stock Company, Dong Hoi, Quangbinh 510000, Vietnam

Orodispersible film (ODF) is a relatively novel oral dosage form that has received considerable attention because of several advantages. Besides rapid drug release and avoidance of first-pass metabolism, it is beneficial for delivering therapeutics in pediatric, geriatric, and patients with swallowing issues and can be administered without water (Hoffmann et al. 2011).

In this study, we developed an ODF formulation incorporating nanoparticulate LOR to enhance the dissolution rate and oral bioavailability of LOR. First, nanoparticulate LOR was prepared and optimized based on the particle size and polydispersity index (PDI). Second, the nanoparticulate LOR was spray-dried along with other additives, dispersed in water, and homogenized. The homogeneous mixture was cast into 6-well plates and dried in an incubator. The resultant film was compared with the pure LOR-incorporated film in terms of physical characteristics such as X-ray diffraction (XRD), differential scanning calorimetry (DSC), SEM, dissolution rate, and bioavailability in rats following oral administration at the LOR dose of 10 mg/kg to confirm its advantages.

## Materials and methods

### Materials

Loratadine was procured from Vasudha Pharma Chem Co., Ltd. (India). Hydroxypropyl methylcellulose (HPMC) E6 and E15 were purchased from Shandong Head Co., Ltd. (China). Polyvinyl pyrrolidone (PVP) K30 was obtained from TNJ Chemical Industry Co., Ltd. (China). Sodium lauryl sulfate (SLS) was obtained from Emery Oleochemicals Marketing, Sdn Bhd (Malaysia). Poloxamer 188 was purchased from Nanning Doublewin Biological Technology Co. Ltd. (China). Polysorbate 80 was purchased from Croda Singapore Pte Ltd. (Singapore). All other chemicals and reagents were of analytical grade and were used without further purification.

### Preparation of loratadine nanoparticles by antisolvent precipitation

The LOR nanoparticles were prepared using the antisolvent precipitation method described previously (Thorat and Dalvi 2012). First, pure LOR was dissolved in ethanol (water-miscible solvent). Second, polymers (HPMC E6, HPMC E15, and PVP K30) and/or surfactants (SLS, poloxamer 188, and polysorbate 80) were dissolved in distilled water (antisolvent). Finally, the drug solutions were dispersed into the aqueous solutions using a syringe at a rate of 120 drops/min. The mixtures were dispersed using a high-shear mixer (IKA RW200, IKA, Germany) at 1500 rpm. The optimized formulation was delivered to a pneumatic nozzle at a flow rate of 1000 mL/h using a spray dryer (SD-1000 Eyela; Eyela, Tokyo, Japan). The process parameters included an input temperature of 160 °C, an air pressure of 10 kPa, and an airflow of 0.6 $m^3$/min. The powder was collected in a plastic bag and stored in a desiccator at room temperature.

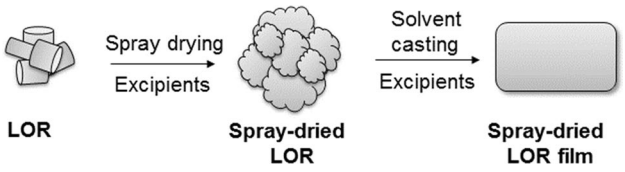


**Scheme 1** Preparations of spray-dried LOR and orodispersible film

### Preparation of orodispersible films

Two ODF formulations were prepared using the solvent casting method (Hoffmann et al. 2011) (Scheme 1). The drug (either pure LOR or nanoparticulate LOR equivalent 5 mg LOR) was weighed, and a film-forming polymer (HPMC E6), surfactant (SLS), plasticizer (glycerol), and saliva stimulant (citric acid) were added at a weight ratio of 5:50:2.5:25:5. The mixture of drug and excipients was dispersed in distilled water and homogenized. The mixtures were continuously stirred in a vacuum for degassing. Subsequently, these mixtures were poured into 6-well plates and allowed to dry overnight at 40 °C in an incubator (Memmert UN110, Memmert GmbH + Co. KG, Germany).

### Physical characterizations

#### Particle size and zeta potential measurements

The particle size, PDI, and zeta potential of the LOR nanoparticles were determined using a nanoPartica SZ-100 nanoparticle analyzer (Horiba, Japan) using a method described previously (Vikash and Kumar 2020). The samples were measured in triplicate following dilution to the appropriate concentrations.

#### Powder X-ray diffraction (PXRD) analysis

The PXRD patterns of pure LOR and nanoparticulate LOR were obtained using an X-ray diffractometer (D8 Advance, Bruker, Germany) following a method described previously (Vasoya et al. 2019). The patterns were recorded at a scanning rate of 1°/min over a range of diffraction angles (2θ) from 5 to 50°.

### Thermal analysis

Thermal analysis of the pure LOR and nanoparticulate LOR was performed using a DSC PT1000 differential scanning calorimeter (Linseis Messgeraete GmbH, Germany) following a method described previously (Albayati et al. 2019). After sealing in aluminum pans, accurately weighed samples (approximately 6 mg) were scanned over a temperature range of 50–250 °C at a heating rate of 10 °C/min under a nitrogen gas flow rate of 50 mL/min.

### FTIR analysis

About 5–10 mg of nanopowder sample was ground finely and then subjected to infrared spectroscopy on a Cary 630 FTIR instrument (Agilent, Malaysia) at wavenumber range of 4000 to 400 $cm^{-1}$ (Tran et al. 2021).

### SEM analysis

The morphologies of loratadine and ODF were observed using an S-4800 scanning electron microscope (Hitachi, Japan) at an accelerating voltage of 10 kV (Truong et al. 2016). The samples were placed onto a double-sided adhesive tape attached to an aluminum stub, and the mounted samples were coated with gold under vacuum.

## Disintegration test

A disintegration test was performed to visually examine the time required for the film to disappear when the film was placed in the buffer solution. Briefly, 20 mL of phosphate buffer (pH 6.8 and 37 °C temperature) was used in the testing conditions. Each film (n = 3) was placed on top of the solution, and the dish was gently shaken until the end of the study.

## Folding endurance

The flexibility of the films was characterized using a folding endurance study. The film was folded repeatedly until it cracked or broke. The folding endurance value was calculated as the number of folding cycles.

## Drug contents

UV–VIS analysis was performed to evaluate the drug content of the films dissolved in 100 mL of methanol. The drug solution was filtered using a 0.45-µm filter before quantification using a UV-2600 UV–VIS Spectrophotometer (Shimadzu, Japan) at an absorption wavelength of 247 nm.

## In vitro drug release studies

The release of pure LOR powder, nanoparticulate LOR powder, pure LOR-loaded film, and nanoparticulate LOR-loaded film was determined in a glass beaker. The nanoparticulate LOR powder was loaded into the capsule, which was subsequently immersed in the dissolution medium using a basket. Samples equivalent to 5 mg of LOR were placed in 20 mL of phosphate buffer solution at pH 6.8, which was maintained at 37 ± 0.5 °C and stirred at a speed of 100 rpm using a C-Mag HS10 magnetic stirrer (IKA, Malaysia). After specific time intervals, the dissolution medium (0.5 mL) was withdrawn and immediately replaced by the same volume of pre-warmed fresh medium (Nguyen et al. 2022). The withdrawn samples were filtered through 0.22-µm membrane filters before determining the concentrations of dissolved LOR using an ultraviolet spectrophotometer UV–2600 (Shimadzu, Japan) at a wavelength of 247 nm.

To compare the dissolution rate of commercialized orodispersible tablets (ODTs), in vitro dissolution studies of loratadine ODT were evaluated using a USP apparatus type I (Basket) at 50 rpm in 900 mL of simulated gastric fluid (SGF) (pH 1.2) without enzyme and at a temperature of 37 ± 0.5 °C. At 2, 4, 6, and 10 min, 10 ml of the solution was aspirated, filtered through a membrane filter, and measured photometrically at 247 nm (Raju et al. 2013). Loratadine SPM 5 mg, a commercialized ODT, was used as a comparative sample.

## Pharmacokinetic studies

The experimental protocols were approved by the Animal Ethical Experimentation Committee of the Vietnam Military Medical University (No. LORA.01 (Hanoi, Vietnam).

Twelve Sprague Dawley rats weighing 180–220 g were randomly divided into two groups (n = 6) and fasted overnight with free access to water before film administration. The nanoparticulate LOR-loaded film and pure LOR-loaded film were orally delivered to rats at 10 mg loratadine/kg dose. At the pre-determined time points (0.25, 0.5, 1, 2, 4, 8, and 24 h), 0.3 mL of blood sample was collected via periorbital puncture and was placed into heparinized tubes. The blood samples were centrifuged at 10,000 rpm for 10 min, followed by a quick vortex. Plasma was separated and stored at − 20 °C until analysis.

The plasma samples were mixed with methanol at 1:1 (*v/v*) ratio. After vortexing for 5 min, the mixture was centrifuged at 18,000 rpm for 15 min at 5 °C. The supernatant was used to analyze LOR concentrations in plasma using the

following procedure. Samples (20 µL) were injected into an Agilent 1260 HPLC system attached to a G1321B fluorescence detector (Agilent, USA). A mobile phase containing acetonitrile:water in 42:58 v/v ratio, which was adjusted to pH 3.0 using phosphoric acid, was eluted through an Eclipse Plus C-18 column (4.6 × 100 mm; 3.5 µm) at a flow rate of 1 mL/min. The effluent was detected at excitation and emission wavelengths of 290 and 460 nm, respectively (Yin et al. 2003).

The pharmacokinetic parameters, including the area under the curve of plasma concentration–time profile from 0 to 24 h ($AUC_{0-24\,h}$), maximum drug concentration ($C_{max}$), time to $C_{max}$ ($T_{max}$), and elimination half-life ($t_{1/2}$), were calculated by non-compartmental analysis using WinNonlin® software version 2.1 (Pharsight, USA).

### Statistical analysis

All experiments were performed in triplicate unless stated otherwise. Results are presented as mean ± standard deviation (SD). The Student's t-test was performed to determine significant differences between the two groups. Statistical significance was set at $p < 0.05$.

## Results and discussion

### Selection of ingredients and parameters for preparation of nanoparticulate loratadine

The LOR nanoparticles were prepared using an antisolvent precipitation method. Pure LOR was dissolved in a water-miscible solvent. Absolute ethanol, which exhibited the highest solubility of LOR, was chosen as the solvent to prepare LOR nanoparticles based on our preliminary study and the results from a previous study (Alshweiat et al. 2018). Water was used as the antisolvent, and the polymer and/or surfactant was dissolved. LOR nanoparticles were optimized by a single-factor design based on particle size and PDI. The factors influencing the nanoparticle formulation process were observed and reported as follows:

#### Effects of the polymer types and percentage

Under the same experimental conditions (drug concentration: 60 mg/mL, solvent/antisolvent ratio: 1/20, and temperature: 25 °C), the effects of polymer types used at 0.2% (*m/v*) were compared. Among the three polymers, HPMC E6 led to the formation of nanoparticles with the smallest particle size and PDI (Fig. 1A). Meanwhile, PVP K30 generated large particles that could be seen by the naked eye (data not shown) since it is less hydrophobic and has fewer functional groups for hydrogen bonding than HPMCs, leading to low adsorption affinity to particle surface (Van Eerdenbrugh et al. 2009; Dalvi and Dave 2009). PVP K30 is also less viscous than HPMCs, resulting in lower stabilization capacity (Sinha et al. 2013). Accordingly, HPMC E6 was selected as the optimal polymer for further studies.

When the concentration of HPMC E6 was increased from 0.2% to 0.6% (w/v), the particle size decreased from 877.0 to 563.9 nm, respectively (Fig. 1B). This might be because higher concentrations of HPMC E6 could decrease the nuclei mobility better, thereby reducing the frequency of collisions between nuclei to form larger particles (Sinha et al. 2013). Thus, 0.6% (*w/v*) of HPMC E6 was selected as the optimal polymer concentration.

#### Effects of drug concentrations

Drug concentrations in the solvent phase affect the degree of supersaturation, thereby affecting nucleation and particle growth rates (Xia et al. 2012). The effects of drug concentrations were studied under the following conditions: 0.6% HPMC E6, solvent/antisolvent ratio of 1/20, mixed using a high-shear mixer at a temperature of 25 ± 0.5 °C. As shown in Fig. 1C, the particle size increased when the drug concentration increased from 20 to 120 mg/mL. This result might be attributed to particle adhesion, agglomeration, and formation of larger particles when a large number of drug nuclei were present at the solvent-antisolvent interface, and the decrease in the diffusion rate of nuclei to the antisolvent phase (Zhang et al. 2009; Sinha et al. 2013). However, PDI values were very high at drug concentrations of 20 and 40 mg/mL (0.821 and 0.972, respectively). Therefore, 60 mg/mL, which showed an acceptable PDI of 0.195 (Danaei et al. 2018), was determined to be the optimal drug concentration.

#### Effects of solvent/antisolvent ratios

The effects of the solvent-to-antisolvent volume ratio (1/20 to 1/100) on particle size and PDI were examined under the same experimental conditions as above. When the ratio decreased from 1/20 to 1/100, the size of the nanoparticles gradually decreased (Fig. 1D) because of an increased degree of supersaturation, resulting in an increased nucleation rate (D'Addio and Prud'homme 2011; Sinha et al. 2013). Thus, 1/100 was selected as the optimal solvent/antisolvent ratio.

#### Effects of surfactant types

Surfactants can adsorb onto particle surfaces, reducing surface tension and increasing nucleation rate. Moreover, adsorption makes the particles more hydrophilic, thereby

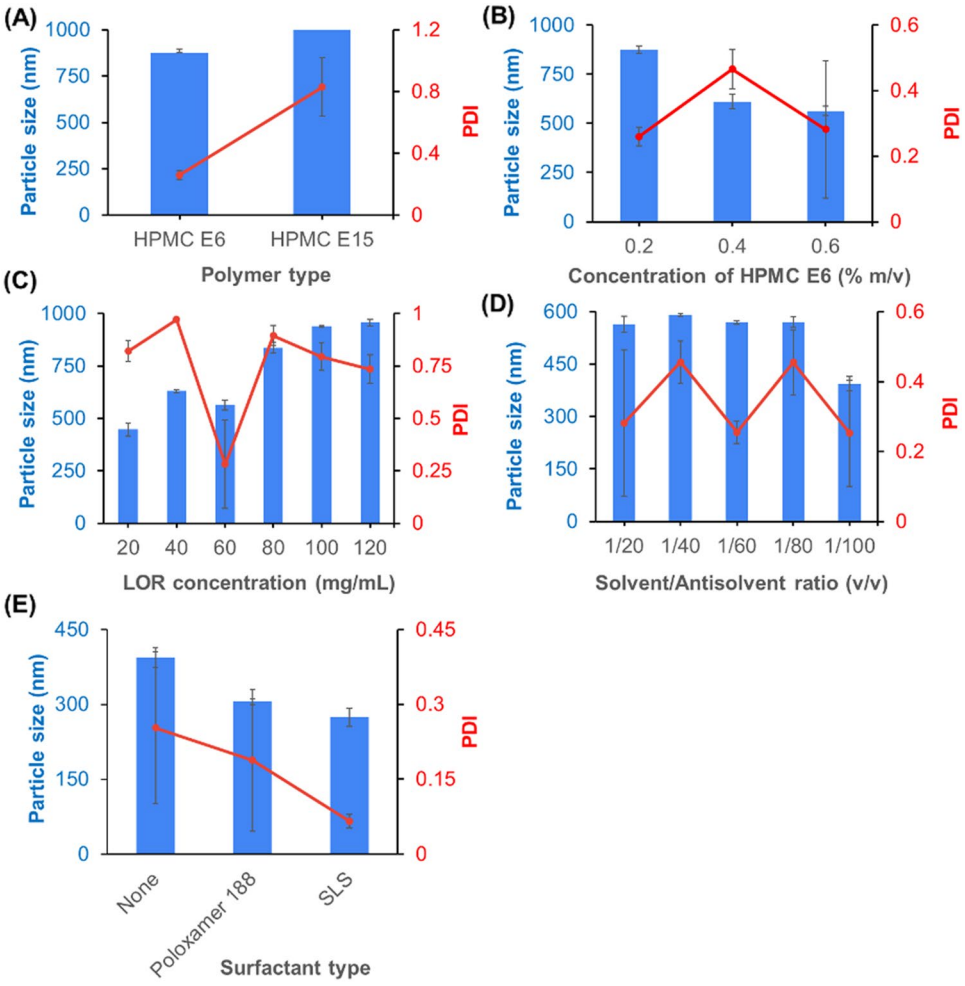


**Fig. 1** The optimization process based on the mean particle size and PDI of LOR nanoparticles. **A** Effects of polymer types. **B** Effects of polymer concentrations. **C** Effects of drug concentrations. **D** Effects of solvent/antisolvent ratios. **E** Effects of surfactant types

decreasing the van der Waals interactions between particles and reducing particle growth (Sinha et al. 2013).

In this study, Poloxamer 188, polysorbate 80, and SLS were used to compare the effects of non-ionic and ionic surfactants on particle size. As expected, anionic SLS supported the formation of nanoparticles with the smallest particle size and PDI, resulting from electrical repulsion (zeta potential of -32.2 ± 0.1 mV) (Fig. 1E). In contrast, the formulation containing non-ionic polysorbate 80 contained large particles that could be seen by the naked eye (data not shown). A possible explanation for this could be the use of a concentration higher than the critical micelle concentration of polysorbate 80, which favors the formation of micelles rather than adsorption on particle surfaces (Deng et al. 2010).

In summary, the optimal formulation was achieved with the following parameters: 0.6% HPMC E6, 0.1% SLS, LOR concentration of 60 mg/mL, and solvent/antisolvent ratio of 1/100 using a high-shear mixer at 1500 rpm at 25 °C. The formulation was spray-dried to form a nanoparticulate powder. The results of characterization studies are provided below.

## Physicochemical characterization

### Powder X-ray diffraction (PXRD) analysis

The PXRD diffractograms of the pure LOR and nanoparticulate LOR are shown in Fig. 2A. Pure LOR showed characteristic peaks at 15.2°, 16.58°, 19.58°, and 21.14°, confirming its crystalline structure. However, these peaks disappeared in the diffractogram of nanoparticulate LOR, suggesting the transformation of LOR into an amorphous state or molecular dispersion of LOR in the carrier matrix.

### Differential scanning calorimetry analysis

The DSC thermogram of pure LOR showed a sharp endothermic peak at 136.1 °C, corresponding to its melting point (Fig. 2B). However, this peak disappeared in the thermogram of nanoparticulate LOR. Therefore, in consensus with the PXRD data, this result confirms that LOR might have changed into an amorphous form or might have molecularly dispersed in the carrier matrix (Zhu et al.

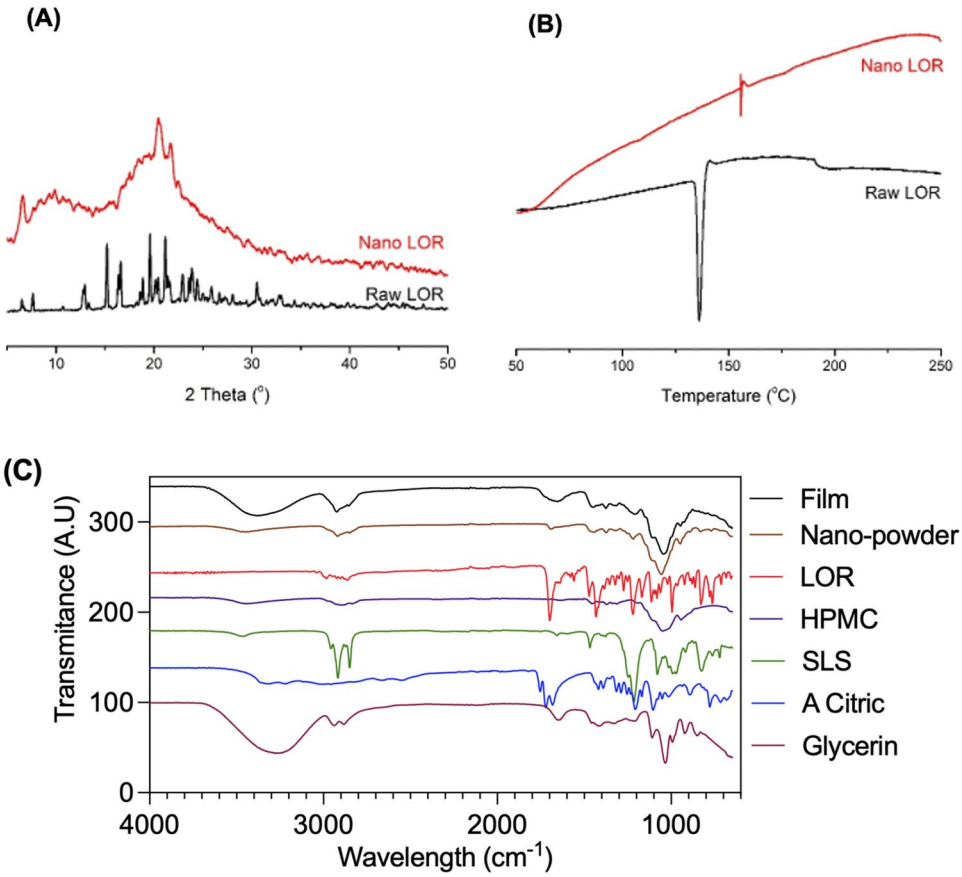


**Fig. 2** **A** PXRD diffractograms and **B** DSC thermograms of pure LOR and nanoparticulate LOR, **C** FTIR spectrum of samples

2010; Melzig et al. 2018). The absence of a thermogram of LOR was also observed in the nanoparticulate LOR-loaded film.

### FTIR analysis

The results of infrared spectrum analysis showed that pure loratadine shows a peak at 995.2 $cm^{-1}$, which is typical for aryl C–Cl bonds; 1222.6 $cm^{-1}$ characterizing the C–N bond of the aryl group of N; the range of 1558.7 $cm^{-1}$ to 1699.7 $cm^{-1}$ characterizing the C–O bond of the amide group or the ester group. The range of 2862.6 $cm^{-1}$ to 2981.9 $cm^{-1}$ is characteristic of C-H bonding (Fig. 2C).

Infrared spectra showed similarities between the spectrum of nanoparticulate loratadine and that of the HPMC E6 polymer. This may be due to the low concentration of loratadine in the nanosystem (approximately 10%) and the high percentage of HPMC E6 (approximately 60%), which led to the characteristic absorption peak of loratadine being obscured by the absorption peak of HPMC E6. The infrared spectrum of nano-loratadine did not show a clear interaction between the drug substance and carrier during the preparation process.

### Other physiochemical properties

SEM images showed the crystalline pattern of the drug, which corresponded to the DSC and XRD results (Fig. 3A). The nanoparticulate LOR-loaded film was depicted as a transparent, regular one containing $4.58 \pm 0.16$ mg of LOR (Fig. 3C, Table 1). The film exhibited a flat surface with various encapsulated materials (Fig. 3D). This film was placed into the medium and disintegrated in 38 s, which is slightly longer than the recommendation (< 30 s) for Orally Disintegrating Tablets in the FDA guidance for industry (Comoglu and Dilek Ozyilmaz 2019).

The film could be folded more than 300 times without any break, indicating the endurance of the film (Table 1). This high flexibility of the film might have resulted from the presence of glycerol and even water with a relatively high amount of plasticizers (Boateng et al. 2009).

## Dissolution studies

The release patterns of LOR in the pure and nanoparticulate powder form are illustrated in Fig. 4A. As can be seen, the release of the drug from pure LOR powder was only 1.4% after the first 5 min and increased slightly to approximately

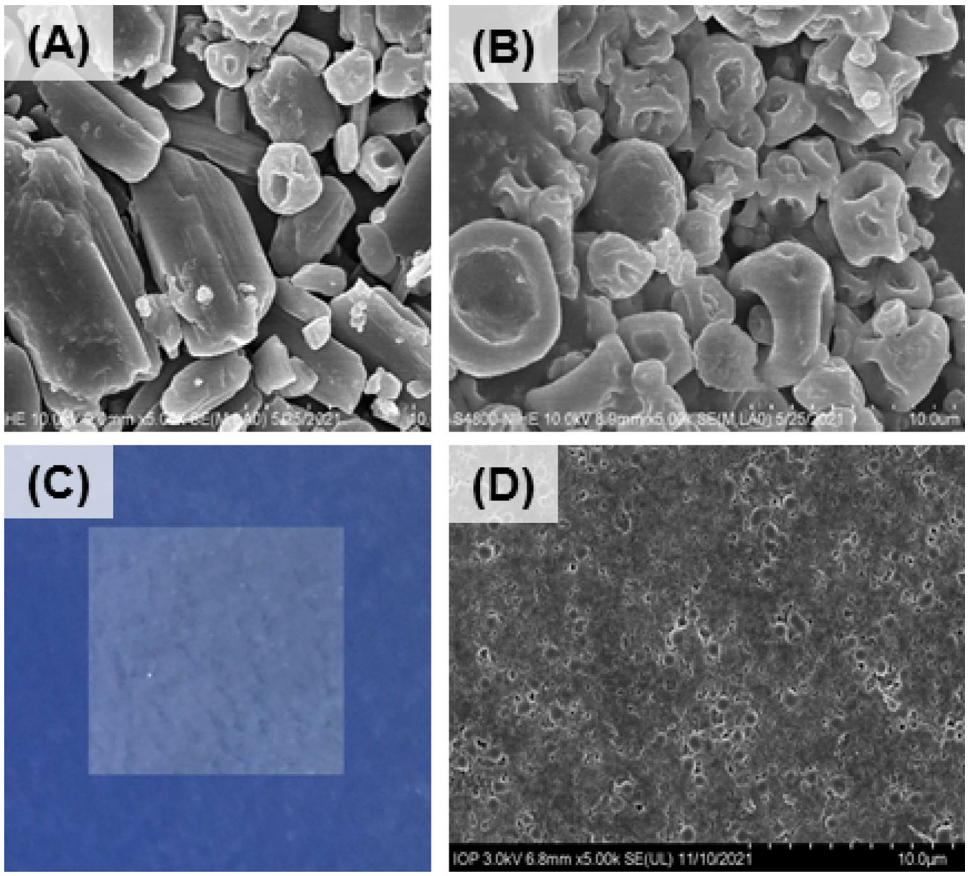


**Fig. 3** SEM analysis of **A** Pure LOR, **B** Spray-dried LOR, **C** Nanoparticulate LOR-loaded film. **D** Spray-dried embedded film

**Table 1** Properties of films

| Film properties (mean ± SD, n = 3) | |
|---|---|
| Disintegrated time (s) | 38 ± 2 |
| Folding endurance | > 300 times |
| Drug content (mg) | 4.58 ± 0.16 |

3.1% after 60 min, which resulted from poor solubility of LOR. In contrast, 7.2% of the drug was released from nanoparticulate LOR powder after 5 min, and the rate dramatically increased to 21.6% after 60 min. This might have been induced by the enhanced surface area and wettability due to the particle size reduction and the presence of the polymer and surfactant on the particle surface. Additionally, the presence of the drug in an amorphous form might help further improve its dissolution rate (Tran et al. 2013; Truong et al. 2015).

Following the encapsulation of drugs into the films, the release of LOR increased to 6.02% and 39.22% for pure LOR-loaded and nanoparticulate LOR-loaded films, respectively, at the end of the experiment (Fig. 4B). This phenomenon might result from the presence of a large percentage of glycerol, which is a water-miscible solvent that can enhance the solubility of poorly soluble LOR.

In our study, the sink conditions were not taken into consideration. First, ODF formulations were administered via the mouth, where the volume of the dissolving medium was too small. Second, LOR is poorly soluble in the dissolution medium and cannot completely dissolve. Finally, sink conditions result in fast release rates of supersaturated formulations that hinder the actual differences between the performances of these formulations (Sun et al. 2016).

The dissolution rate of LOR in the nanoparticulate LOR-loaded film was compared with that of the commercialized ODT in media without the enzyme. As shown in Fig. 4C, after 10 min, approximately 90% of the drug was released from both formulations, indicating the availability for the adsorption and the similarity between both formulations (Diaz et al. 2016). Therefore, the nanoparticulate LOR-loaded film met the requirement for a quick-release dosage form.

## Pharmacokinetic study

The pharmacokinetic profiles of the two LOR-loaded ODF formulations following oral administration to rats are shown in Fig. 5. The corresponding pharmacokinetic parameters are listed in Table 2. The nanoparticulate LOR-loaded formulation demonstrated significantly higher $C_{max}$

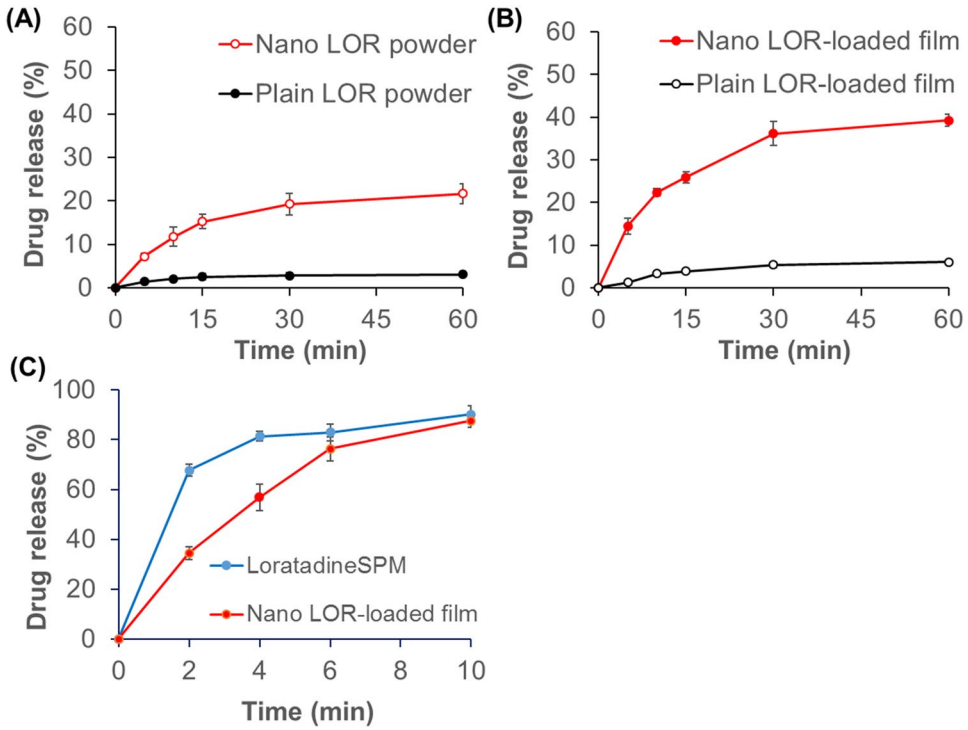


**Fig. 4** Release profiles of LOR from **A** Powder forms and **B** Drug-loaded films. **C** Dissolution profiles of LOR from the nanoparticulate LOR-loaded film and the commercialized orodispersible tablet Loratadine SPM

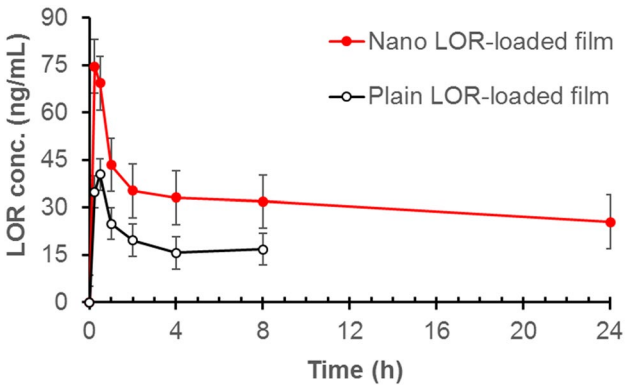


**Fig. 5** Plasma concentration–time profiles of LOR after oral administration of orodispersible films containing pure LOR and nanoparticulate LOR in rats

**Table 2** Pharmacokinetic parameters of LOR after oral administration of orodispersible films containing pure LOR and nanoparticulate LOR in rats (mean ± SD, n = 6)

| Parameters | Pure LOR-loaded films | Nanoparticulate LOR-loaded films |
|---|---|---|
| $C_{max}$ (ng/mL) | 42.56 ± 4.21 | 76.86 ± 15.04*** |
| $T_{max}$ (h) | 0.38 ± 0.14 | 0.29 ± 0.10 |
| $AUC_{0\text{-}24\,h}$ (h.ng/mL) | 128.72 ± 61.64 | 751.11 ± 78.46*** |
| $t_{1/2}$ (h) | 5.14 ± 2.46 | 26.23 ± 11.63** |

**p < 0.01; ***p < 0.001, compared to pure LOR-loaded films

and $AUC_{0\text{-}24\,h}$ than those of the pure LOR-loaded counterpart (p < 0.001). Specifically, $C_{max}$ (76.86 ± 15.04 ng/mL) and $AUC_{0\text{-}24\,h}$ (751.11 ± 78.46 h.ng/mL) of the nanoparticulate LOR-loaded formulation were approximately 1.8-fold and 5.8-fold higher than those of the other, respectively. Additionally, the elimination half-life of the nanoparticulate LOR-loaded formulation (26.23 ± 11.63 h) was 5.1-fold higher than that of the pure LOR-loaded formulation (p < 0.01), suggesting that this formulation could help reduce the frequency of drug administration, thereby promoting patient compliance.

## Conclusion

In this study, orodispersible films incorporating nanoparticulate LOR, a BCS class II drug, were successfully prepared. Nanoparticulate LOR was prepared using antisolvent precipitation, followed by spray drying. Not only did the nanoparticulate LOR-loaded orodispersible film exhibit a significantly higher release rate and oral bioavailability of LOR, but it also showed a longer half-life compared to the pure LOR-loaded orodispersible film. These results suggest the possibility of using orodispersible films to enhance the oral bioavailability of poorly water-soluble drugs and to improve patient compliance.

## Declarations

**Conflict of interest** All authors (Khanh Van Nguyen, Thu Kim Dang, Linh Thi Dieu Vu, Nhan Thi Ha, Hieu Duy Truong, and Tuan Hiep Tran) declare that they have no conflict of interest.

**Statement of human and animal rights** Animal studies were performed after receiving approval from the Animal Ethics Experimentation Committee of Vietnam Military Medical University No. LORA.01 (Hanoi, Vietnam).

**Availability of Data and Materials** The authors confirm that the data supporting the findings of this study are available within the article and its supplementary materials. The data that support the findings of this study are available from the corresponding author, on special request.

## References


Albayati TM, Salih IK, Alazzawi HF (2019) Synthesis and characterization of a modified surface of SBA-15 mesoporous silica for a chloramphenicol drug delivery system. Heliyon 5:e02539

Alshweiat A, Katona G, Csóka I, Ambrus R (2018) Design and characterization of loratadine nanosuspension prepared by ultrasonic-assisted precipitation. Eur J Pharm Sci 122:94–104

Boateng JS, Stevens HNE, Eccleston GM et al (2009) Development and mechanical characterization of solvent-cast polymeric films as potential drug delivery systems to mucosal surfaces. Drug Dev Ind Pharm 35:986–996

Comoglu T, Dilek Ozyilmaz E (2019) Orally disintegrating tablets and orally disintegrating mini tablets—novel dosage forms for pediatric use. Pharm Dev Technol 24:902–914

D'Addio SM, Prud'homme RK (2011) Controlling drug nanoparticle formation by rapid precipitation. Adv Drug Deliv Rev 63:417–426

Dalvi SV, Dave RN (2009) Controlling particle size of a poorly water-soluble drug using ultrasound and stabilizers in antisolvent precipitation. Ind Eng Chem Res 48:7581–7593

Danaei M, Dehghankhold M, Ataei S et al (2018) Impact of particle size and polydispersity index on the clinical applications of lipidic nanocarrier systems. Pharmaceutics 10:57

Deng J, Huang L, Liu F (2010) Understanding the structure and stability of paclitaxel nanocrystals. Int J Pharm 390:242–249

Desai P, Wang KZ, Ann D et al (2020) Efficacy and pharmacokinetic considerations of loratadine nanoformulations and its combinations for pancreatic cancer chemoprevention. Pharm Res 37:21

Diaz DA, Colgan ST, Langer CS et al (2016) Dissolution similarity requirements: how similar or dissimilar are the global regulatory expectations? AAPS J 18:15–22

Frizon F, de Oliveira EJ, Donaduzzi CM et al (2013) Dissolution rate enhancement of loratadine in polyvinylpyrrolidone K-30 solid dispersions by solvent methods. Powder Technol 235:532–539

Hoffmann EM, Breitenbach A, Breitkreutz J (2011) Advances in orodispersible films for drug delivery. Expert Opin Drug Deliv 8:299–316

Kapote DN, Wagner KG (2021) Influence of shellac on the improvement of solubility and supersaturation of loratadine amorphous solid dispersion using a new grade of HPMC. J Drug Deliv Sci Technol 61:102116

Khan MZI, Raušl D, Zanoški R et al (2004) Classification of loratadine based on the biopharmaceutics drug classification concept and possible *in Vitro–in Vivo* Correlation. Biol Pharm Bull 27:1630–1635

Madhav KV, Kishan V (2018) Self microemulsifying particles of loratadine for improved oral bioavailability: preparation, characterization and in vivo evaluation. J Pharm Investig 48:497–508

Melzig S, Finke JH, Schilde C, Kwade A (2018) Formation of long-term stable amorphous ibuprofen nanoparticles via antisolvent melt precipitation (AMP). Eur J Pharm Biopharm 131:224–231

Nguyen KV, Dang TK, Pham HT et al (2022) Development of Panax notoginseng saponins-loaded orodispersible films: a potential approach to enhance delivery efficacy in older adults. J Appl Pharm Sci 12:44–53

Raju PN, Kumar MS, Reddy CM, Ravishankar K (2013) Formulation and evaluation of fast dissolving films of loratidine by solvent casting method. Pharma Innov 2:5

Roman IJ, Danzig MR (1993) Loratadine. a review of recent findings in pharmacology, pharmacokinetics, efficacy, and safety, with a look at its use in combination with pseudoephedrine. Clin Rev Allergy 11:89–110

Sarheed O, Shouqair D, Ramesh K et al (2020) Physicochemical characteristics and in vitro permeation of loratadine solid lipid nanoparticles for transdermal delivery. Ther Deliv 11:685–700

Sinha B, Müller RH, Möschwitzer JP (2013) Bottom-up approaches for preparing drug nanocrystals: Formulations and factors affecting particle size. Int J Pharm 453:126–141

Sora DI, Udrescu S, David V, Medvedovici A (2007) Validated ion pair liquid chromatography/fluorescence detection method for assessing the variability of the loratadine metabolism occurring in bioequivalence studies. Biomed Chromatogr 21:1023–1029

Sun DD, Wen H, Taylor LS (2016) Non-sink dissolution conditions for predicting product quality and in vivo performance of supersaturating drug delivery systems. J Pharm Sci 105:2477–2488

Thorat AA, Dalvi SV (2012) Liquid antisolvent precipitation and stabilization of nanoparticles of poorly water soluble drugs in aqueous suspensions: recent developments and future perspective. Chem Eng J 181–182:1–34

Tran TH, Poudel BK, Marasini N et al (2013) Preparation and evaluation of raloxifene-loaded solid dispersion nanoparticle by spray-drying technique without an organic solvent. Int J Pharm 443:50–57

Tran TB, Tran TH, Vu YH et al (2021) pH-responsive nanocarriers for combined chemotherapies: a new approach with old materials. Cellulose 28:3423–3433

Truong DH, Tran TH, Ramasamy T et al (2015) Preparation and characterization of solid dispersion using a novel amphiphilic copolymer to enhance dissolution and oral bioavailability of sorafenib. Powder Technol 283:260–265

Truong DH, Tran TH, Ramasamy T et al (2016) Development of solid self-emulsifying formulation for improving the oral bioavailability of erlotinib. AAPS PharmSciTech 17:466–473

Üner M, Karaman EF, Aydoğmuş Z (2014) Solid Lipid nanoparticles and nanostructured lipid carriers of loratadine for topical application: physicochemical stability and drug penetration through rat skin. Trop J Pharm Res 13:653–660

Van Eerdenbrugh B, Van den Mooter G, Augustijns P (2008) Top-down production of drug nanocrystals: nanosuspension stabilization, miniaturization and transformation into solid products. Int J Pharm 364:64–75

Van Eerdenbrugh B, Vermant J, Martens JA et al (2009) A screening study of surface stabilization during the production of drug nanocrystals. J Pharm Sci 98:2091–2103

Vasoya JM, Desai HH, Gumaste SG et al (2019) Development of solid dispersion by hot melt extrusion using mixtures of polyoxylglycerides with polymers as carriers for increasing dissolution rate of a poorly soluble drug model. J Pharm Sci 108:888–896

Vikash, Kumar V (2020) Ultrasonic-assisted de-agglomeration and power draw characterization of silica nanoparticles. Ultrason Sonochem 65:105061

Wang J, Chang R, Zhao Y et al (2017) Coamorphous loratadine-citric acid system with enhanced physical stability and bioavailability. AAPS PharmSciTech 18:2541–2550

Wu L, Zhang J, Watanabe W (2011) Physical and chemical stability of drug nanoparticles. Adv Drug Deliv Rev 63:456–469

Xia D, Wu JX, Cui F et al (2012) Solvent-mediated amorphous-to-crystalline transformation of nitrendipine in amorphous particle suspensions containing polymers. Eur J Pharm Sci 46:446–454

Yin OQP, Shi X, Chow MSS (2003) Reliable and specific high-performance liquid chromatographic method for simultaneous determination of loratadine and its metabolite in human plasma. J Chromatogr B 796:165–172

Zhang H-X, Wang J-X, Zhang Z-B et al (2009) Micronization of atorvastatin calcium by antisolvent precipitation process. Int J Pharm 374:106–113

Zhu W-Z, Wang J-X, Shao L et al (2010) Liquid antisolvent preparation of amorphous cefuroxime axetil nanoparticles in a tube-in-tube microchannel reactor. Int J Pharm 395:260–265